Spatio-Temporal Coding in Complex Media for Optimum Beamforming: The Iterative Time-Reversal Approach

Gabriel Montaldo, Jean-François Aubry, Mickaël Tanter, and Mathias Fink

***Abstract*—Spatio-temporal encoding in transmit and receive modes is of major importance in the development of ultrasound imaging devices. Classically, the assumption of constant sound speed in the medium allows one to restrict the beamforming process to the application of a cylindrical time-delay law on the elements of a multiple-transducer array. Here is proposed an iterative time-reversal method capable of taking into account all the heterogeneities of the medium, concerning density, speed of sound, and absorption variations. It will be shown that this iterative focusing process converges toward a spatio-temporal inverse filter focusing, the first step of the process being a time-reversal focusing on the targeted point. This method can be seen as a calibration process and has been successfully applied to transskull focusing and intraplate echoes suppression. It is leading the way to promising applications such as high-resolution ultrasonic brain imaging and high-resolution focusing through complex reverberating media, in nondestructive testing and telecommunications. This work highlights the advantages of using spatio-temporal coding to focus through complex media. Such codes require the use of fully programmable, multichannel electronics to implement this technique in real time.**

I. Introduction

In conventional ultrasonic imaging devices, the beamforming is achieved by assuming constant acoustical properties of the medium under investigation. However, plates or screws may affect the focusing in nondestructive testing. In medical imaging, tissue heterogeneities exist and degrade the ultrasonic focused beam as shown extensively during the past decades [1]–[3]. In order to correct these distortions, the aberrations were first modeled as a very thin layer introducing varying time delays along the array aperture. Time shifts have been proposed to compensate the effect of the aberrating layer, assuming that this layer is located close to the array [4] or at a given distance [5]. In this case, the same temporal coding is applied on each channel: short pulses with varying phases and amplitudes. Recently, more complex temporal codes (coded excitations [6]) have been successfully implemented to increase the sensitivity of commercial imaging devices. Again, an identical temporal coding is applied on each channel of the device.

However, as the heterogeneities are dispersed in the whole insonified area, different temporal codes theoretically should be applied on each element of the emitting array, requiring fully programmable transducers. If the absorption coefficient of the medium is low or nearly uniform, time reversal is a fast and robust way to compensate the distortions induced by the medium, as it corresponds to the inverse filter of the propagation operator. This technique was the first spatio-temporal coding used to focus through complex media [7], [8]. It is now intensively studied, especially in nondestructive testing [9], ultrasonic therapy, in under water acoustic communications [10], [11], and in wireless communications [12].

Nevertheless, in an heterogeneous lossy medium, one has to go beyond time reversal as it corresponds only to a spatial and temporal matched filter of the propagation operator [13]: the time-reversal process maximizes the pressure amplitude received at focus but does not impose any constraints on the field around the focus, so that the focusing pattern obtained in the focal plane is not optimum any more in heterogeneous absorbing media. In order to construct the inverse filter in a lossy medium, the whole propagation operator relating the transducer array to a set of control points surrounding the desired focus has to be acquired. In fact, this propagation operator acts as a spatio-temporal filter on the emitted signals, and its inversion allows recovering the optimal focusing on a desired point of the control plane [14]. Ebbini and Cain [15] first introduced in 1989 a set of control points surrounding the focus in order to achieve multiple focus synthesis for hyperthermia treatments by using a pseudo inversion of the propagation matrix. In 1994, they used the same method to perform phase aberration correction for hyperthermia [16]. In previous works, Tanter *et al.* and Aubry *et al.* introduced a singular value decomposition of the propagation operator, minimizing the error between the desired focus and the obtained focus, and extended the method to broadband focusing through reverberating and absorbing media [14]. Aubry *et al.* [17] also showed that, thanks to the spatial reciprocity of the propagation operator, receive encoding can be deduced from transmit encoding leading the way to transmit and receive focusing with the inverse-filter technique. Note that these techniques are based on the use

Manuscript received December 31, 2003; accepted June 10, 2004. This work was supported by grant QLG1-CT-2002-01518 (UMEDS: Ultrasonographic Monitoring and Early Diagnosis of Stroke) from the European Commission.

The authors are with Laboratoire Ondes et Acoustique, Ecole Supérieure de Physique et de Chimie Industrielles de la Ville de Paris (ESPCI), Université Denis Diderot, Centre National de la Recherche Scientifique (CNRS UMR 7587), 75231 Paris Cedex 05, France (e-mail: jean-francois.aubry@espci.fr).

of receivers in the focal plane. This configuration is well suited for telecommunications but not applicable directly in most practical situations for medical imaging or nondestructive testing. However, in such cases, this inverse-filter technique has to be seen as a precalibration process. But achieving this precalibration process experimentally allows, for example, the improvement of arrays performances [13] or unwanted reverberations cancellations while imaging through plates [14]. However, this calibration process also can be coupled to numerical simulations for beam patterns optimizations. In this second type of calibration processing, Ranganathan and Walker [18], [19] revisited these concepts recently with the so-called minimum sum squared error (MSSE). All these studies demonstrated the advantage of inverting the propagation operator to focus through complex media.

The drawback of these powerful focusing methods based on the inversion of the propagation operator is that they are time consuming: the propagation operator first has to be recorded, then a delicate numerical inversion has to be computed on an ill-conditioned operator.

It is shown in this paper that all these techniques developed for ultrasonic imaging and therapy, based on the inversion of the propagation operator, can be achieved with a hardware iterative process without numerical calculation of the inverse of the propagation operator. This iterative focusing technique was introduced recently [20] and is based on an iterative time-reversal process. One has to note that adjoint methods mathematically act in a similar way: Norton [21] nicely discussed how iterative inverse scattering can be conducted thanks to the forward problem and only one adjoint solution, so that the method proposed here could have interesting echoes in inverse-scattering theories in various fields, such as characterization of material or seismology.

In Section II, the interpretation of the time-reversal technique and the inverse filter in terms of propagation operators is introduced. Their respective focusing capabilities are compared through two different media: a human skull and a solid plate. The human skull has been chosen because of its high heterogeneous absorption. Enhancing transskull focusing could have a strong impact on future ultrasonic brain imaging devices. The solid plate model is an academic model presenting multiple reflections as the ones that occur through coupling windows which occurs in medical as well as in nondestructive testing.

The iterative process is then explained and tested on both media. It is shown that this technique exhibits a step-by-step transition from time reversal to inverse filter. The various coding techniques are compared using the spatio-temporal shape of the emitting vectors and the corresponding spatio-temporal focusing measured in the focal plane. Such a hardware iterative process is a lot less time consuming as it does not require acquiring the entire propagation operator relating the array to the control points and can be implemented in real time as the duration of each step corresponds only to a back-and-forth propagation between the arrays. This iteration achieves the inverse filter in an experimental way, using waves propagation instead of computational power.

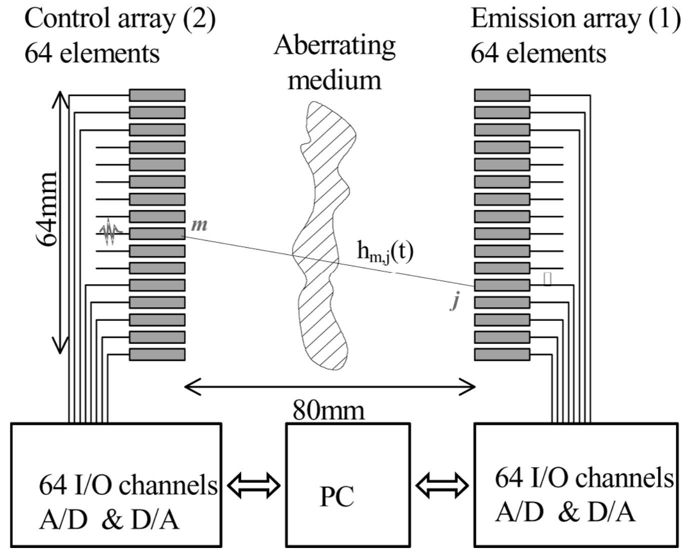

Fig. 1. Experimental set-up: an aberrating medium is located between 64 control points and an emitting array of 64 transducers.

II. Time Reversal and the Propagation Operator

A. The Propagation Operator $h_{mj}(t)$

We define the linear operator relating the elements of the transducer array to a set of control points embedded in the medium. The signals applied to the transducer elements are the input of the linear operator, and the output consists of the signals measured on the control points.

For simplicity, we restrict ourselves to a one-dimensional array of transducers and a one-dimensional set of control points along a line parallel to the array aperture. Basically, the experimental setup is composed of two arrays of transducers facing each other and separated by the aberrating medium under investigation, as shown in Fig. 1. The arrays are made of 64 elements working at a 1.5 MHz central frequency with a 70% bandwidth. Each element is connected to its own input/output fully programmable electronic channel.

For each couple (control point m, transducer j), we define the impulse response $h_{mj}(t)$, which corresponds to the signal received on the m^{th} control point after a temporal Dirac function is applied on the j^{th} transducer of the array. This response includes all the propagation effects through the considered medium as well as the acoustoelectric responses of the two elements. Each impulse response is acquired experimentally. This set of $N \times N$ temporal functions characterizes the propagation operator. Let $e_j(t)$, $1 \leq j \leq N$, be the input signal on the j^{th} transducer. As the effects of the propagation in the medium are supposed linear and invariant under a time shift, the output signal $f_m(t)$, $1 \leq m \leq N$, received on the m^{th} control point is given by:

$$f_m(t) = \sum_{j=1}^{N} h_{mj}(t) \otimes e_j(t),\ 1 \leq m \leq N, \qquad (1)$$

where $\otimes$ is a temporal convolution operator.

A temporal Fourier transform leads to the following relation:

$$F_m(\omega) = \sum_{j=1}^{N} \mathbf{H}_{mj}(\omega) E_j(\omega),\ 1 \leq m \leq N, \qquad (2)$$

(2) can be written in a matrix form:

$$F(\omega) = \mathbf{H}(\omega) E(\omega), \qquad (3)$$

where $E(\omega) = (E_j(\omega))_{1 \leq j \leq N}$ is a complex column vector corresponding to the Fourier transform of the emitted signals and $F(\omega) = (F_m(\omega))_{1 \leq m \leq N}$ is a complex column vector of the Fourier transform of the received signals. The transfer matrix $\mathbf{H}(\omega) = \{H_{mj}(\omega)\}_{1 \leq m \leq N,\, 1 \leq j \leq N}$ describes the propagation in the medium from the array to the set of control points for a chosen frequency component and thus is called the monochromatic propagation matrix [13]. Due to spatial reciprocity, the nonconjugate transpose of the transfer matrix ${}^t\mathbf{H}(\omega) = \{H_{jm}(\omega)\}_{1 \leq m \leq N,\, 1 \leq j \leq N}$ describes the propagation in the medium from the set of control points to the array for a chosen frequency component. In this paper, ^{t} denotes the nonconjugate transpose operator.

B. Time-Reversal Operation: Matrix Formulation

In a time-reversal mirror experiment, an impulse pressure field generated by an acoustic source is recorded after propagation on an array of transducers. The recorded signals are time reversed and transmitted simultaneously. In a lossless propagation medium, as the wave equation remains unchanged under a time-reversal transform, the time-reversed signal will focus back to the initial point source as if the film of the propagation was played backward. This process can be interpreted in a matrix formalism.

In a first step, an impulse is emitted by a source located on one of the control points. This corresponds to an emission vector $s(t) = [0, \dots 0, s_i(t), 0, \dots, 0]$, with $s_i(t) = \delta(t)$ being a temporal dirac function. We denote $S(\omega) = [0, \dots 0, 1, 0, \dots, 0]$, the Fourier transform of $s(t)$. The signals received by the elements of array 1 (see Fig. 1), $R(\omega)$ are given by:

$$R(\omega) = {}^t\mathbf{H}(\omega) S(\omega). \qquad (4)$$

The received signals then are time reversed and reemitted through the propagation operator, so that the signals $F(\omega)$ received in the focal plane on the control points are given by:

$$F(\omega) = \mathbf{H}(\omega) R^* = \mathbf{H}(\omega)\mathbf{H}^\dagger(\omega) S^*(\omega), \qquad (5)$$

where † denotes the transpose conjugate operator.

As $S^*(\omega) = [0, \dots 0, 1, 0, \dots, 0]$, one can see that the result of the time-reversal focalization on the i^{th} control point is plotted along the i^{th} line of the $\mathbf{H}(\omega)\mathbf{H}^\dagger(\omega)$ matrix, the so-called time-reversal matrix. Similarly, the result of the time-reversal focalization on the j^{th} emitting point is plotted along the j^{th} column of the $\mathbf{H}(\omega)\mathbf{H}^\dagger(\omega)$ matrix. An optimum focusing is obtained on the focal point if this matrix is equal to the identity matrix within the diffraction limit.

This $\mathbf{H}(\omega)\mathbf{H}^\dagger(\omega)$ matrix is given in Fig. 2 at the central frequency for two different propagation media: in water without any aberrator [Fig. 2(a)] and through a human skull [Fig. 2(b)]. The focusing in water gives a reference; due to diffraction limits, this matrix is not equal to the identity matrix but is quite close. One can see that, in the case of a heterogeneous absorbing medium like a human skull, time reversal cannot restore a good focusing. In order to improve the focusing, one has to invert the propagation operator to compensate the losses induced by the aberrating medium.

III. Inverting the Propagation Operator

The propagation operator acts as a spatio-temporal filter on the emitted signals. In order to recover the components that have been filtered by the medium, one has to invert this filter. The aim is to determine the desired emission vector $E(\omega)$ that has to be emitted by the array 1 in order to give rise after propagation to the signal previously emitted in the first step of the time-reversal experiment: $S(\omega) = [0, \dots 0, S_i\omega) = 1, 0, \dots, 0]$.

According to (3), $E(\omega)$ and $S(\omega)$ are related by:

$$S(\omega) = \mathbf{H}(\omega)\, E(\omega) \Leftrightarrow E(\omega) = \mathbf{H}^{-1}(\omega) S(\omega). \qquad (6)$$

As is the case in all inverse problems, the inversion of the propagation matrix $\mathbf{H}$ is ill-conditioned [22]. A regularization of the inversion can be performed by computing the singular value decomposition of the matrix $\mathbf{H}(\omega)$ before inversion:

$$\mathbf{H}(\omega) = \mathbf{U}(\omega)\mathbf{D}(\omega)\mathbf{V}^\dagger(\omega), \qquad (7)$$

here, $\mathbf{D}(\omega)$ is a diagonal matrix of singular values (arranged in decreasing order) and $\mathbf{U}(\omega)$ and $\mathbf{V}(\omega)$ are unitary matrices.

The matrix inversion is applied only to the main (i.e., physically relevant) singular vectors of the singular value decomposition of $\mathbf{H}(\omega)$. It gives rise to a noise-filtered approximation $\tilde{\mathbf{H}}^{-1}(\omega)$ of the inverse matrix $\mathbf{H}^{-1}(\omega)$:

$$\begin{aligned}\tilde{\mathbf{H}}^{-1}(\omega) &= \mathbf{V}(\omega)\hat{\mathbf{D}}^{-1}(\omega)\mathbf{U}^\dagger(\omega)\\ &= \mathbf{V}(\omega)\begin{bmatrix}\lambda_1(\omega)^{-1} & 0 & \cdots & \cdots\cdots & 0\\ 0 & \ddots & 0 & & \vdots\\ \vdots & 0 & \lambda_{N_0}(\omega)^{-1} & 0 & \vdots\\ \vdots & & & \ddots & \vdots\\ 0 & \cdots & \cdots & \cdots\cdots & 0\end{bmatrix}\mathbf{U}^\dagger(\omega),\end{aligned} \qquad (8)$$

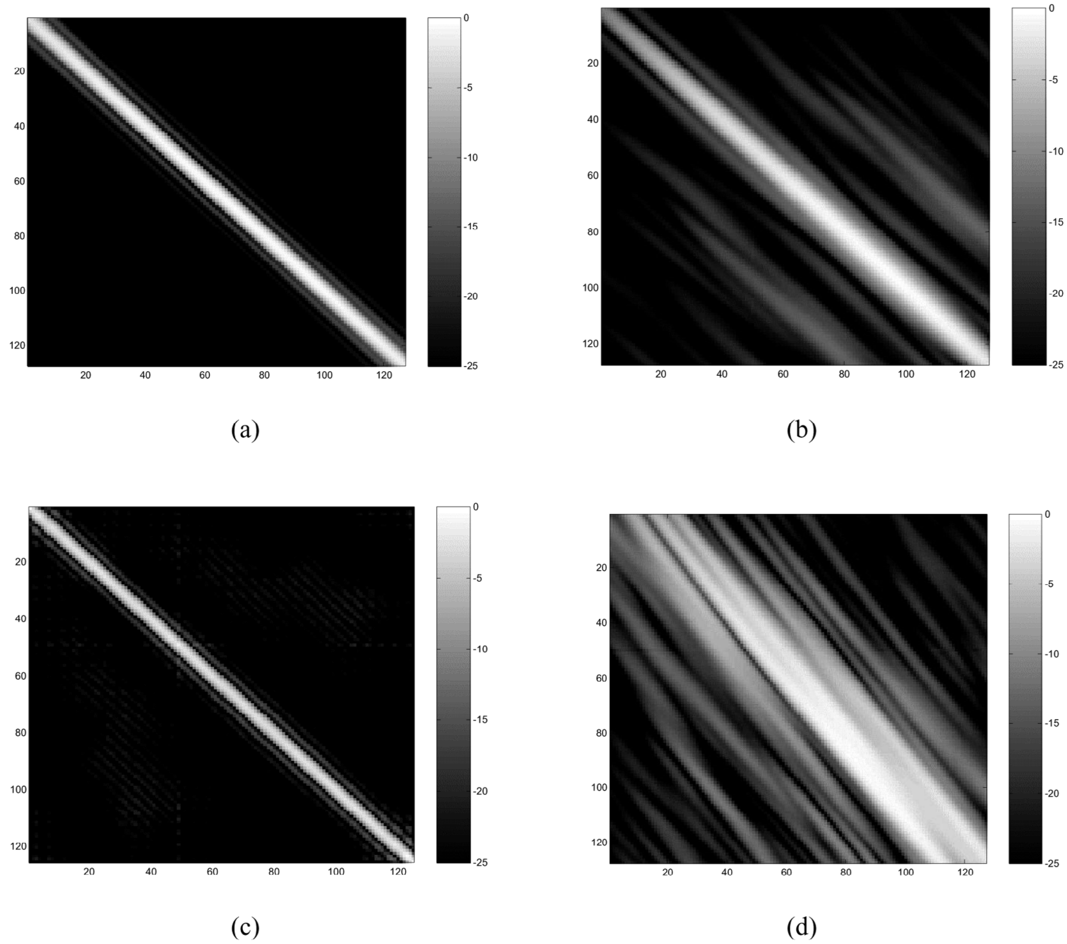

Fig. 2. Focusing capabilities of various techniques: (a) $\mathbf{H_{water}}(\omega)^{\mathbf{t}}\mathbf{H^*_{water}}(\omega)$: time reversal in water. (b) $\mathbf{H_{skull}}(\omega)^{\mathbf{t}}\mathbf{H^*_{skull}}(\omega)$: time reversal through a human skull. (c) $\mathbf{H_{skull}}(\omega)\tilde{\mathbf{H}}^{-1}_{\mathbf{skull}}(\omega)$: inverse filter through a human skull. (d) $\mathbf{H_{skull}}(\omega)^{\mathbf{t}}\mathbf{H^*_{water}}(\omega)$: cylindrical law through a human skull.

where N_0 is the number of physically relevant singular values [13]. The last $N - N_0$ singular values corresponds to noise and are not inverted but definitely set to zero.

Once $\tilde{\mathbf{H}}^{-1}(\omega)$ has been calculated, the monochromatic part of the emission signal at the given frequency can be determined:

$$E(\omega) = \tilde{\mathbf{H}}^{-1}(\omega)S(\omega), \tag{9}$$

$E(\omega)$ is emitted though the propagation operator, so that the signals $F(\omega)$ received in the focal plane at the control points are given by:

$$F(\omega) = \mathbf{H}(\omega)E(\omega) = \mathbf{H}(\omega)\tilde{\mathbf{H}}^{-1}(\omega)S(\omega). \tag{10}$$

As $S(\omega) = [0, \ldots 0, 1, 0, \ldots, 0]$, one can see that the result of the inverse-filter focalization on the i^{th} control point is plotted along the i^{th} line of the $\mathbf{H}(\omega)\tilde{\mathbf{H}}^{-1}(\omega)$ matrix. Similarly, the result of the inverse-filter focalization on the j^{th} emitting point is plotted along the j^{th} column of the $\mathbf{H}(\omega)\tilde{\mathbf{H}}^{-1}(\omega)$ matrix. This matrix is equal to the identity matrix limited to the subspace of the physical relevant singular vectors:

$$\begin{aligned} F(\omega) &= \mathbf{H}(\omega)\tilde{\mathbf{H}}^{-1}(\omega)S(\omega) \\ &= \mathbf{U}(\omega)\begin{bmatrix} 1 & 0 & \cdots & \cdots & \cdots & 0 \\ 0 & \ddots & 0 & & & \vdots \\ \vdots & 0 & 1 & & & \vdots \\ \vdots & & & 0 & & \vdots \\ \vdots & & & & \ddots & \vdots \\ 0 & \cdots & \cdots & \cdots & \cdots & 0 \end{bmatrix}\mathbf{U}^{\dagger}(\omega)S(\omega). \end{aligned} \tag{11}$$

This $\mathbf{H}(\omega)\tilde{\mathbf{H}}^{-1}(\omega)$ matrix is given in Fig. 2(c) at the central frequency when focusing through a human skull. One can see that the focusing quality is now optimum whatever the position of the focus. This representation gives a quick overview of the effectiveness of the focusing method under investigation. Similarly, one can compare the focusing obtained through a human skull by using a cylindrical law. In that case, the emitted signals correspond to the propagation of impulses through water. In order to prevent any confusion, we will denote $\mathbf{H_{skull}}(\omega)$ as the propagation matrix through the skull from array 1 to array 2 and $\mathbf{H_{water}}(\omega)$ the propagation matrix in water from array 1 to array 2. The cylindrical signals are given by:

$$E(\omega) = {}^t\mathbf{H_{water}}(\omega)S(\omega). \tag{12}$$

And the signals $F(\omega)$ received in the focal plane at the control points are given by:

$$F(\omega) = \mathbf{H_{skull}}(\omega)E(\omega) = \mathbf{H_{skull}}(\omega){}^t\mathbf{H_{water}}(\omega)S(\omega). \tag{13}$$

With cylindrical laws, the focalization on the i^{th} control point is plotted along the i^{th} line of the $\mathbf{H_{skull}}(\omega){}^t\mathbf{H_{water}}(\omega)$ matrix. Similarly, the result of the inverse-filter focalization on the j^{th} emitting point is in fact plotted along the j^{th} column of the $\mathbf{H_{skull}}(\omega){}^t\mathbf{H_{water}}(\omega)$ matrix. This matrix is given in Fig. 2(d) at the central frequency when focusing through a human skull. One can see the strong impact of the skull: contrary to time-reversal and inverse-filter focusing, the maximum of the matrix is not located on the diagonal, resulting in a distortion of the image (refraction effects of the skull).

IV. Extension to Broadband Focusing

Naturally, this monochromatic study can be extended to broadband focusing by performing it at each frequency and by combining them back with an inverse Fourier transform. For example, the optimal set of broadband emission signals $\{e_j(t)\}$ is simply deduced from $E_j(\omega)$ by:

$$e_j(t) = \mathbf{F}^{-1}\left(E_j(\omega)\right) = \int_{\omega} E_j(\omega)e^{-i\omega t}d\omega,\ 1 \leq m \leq N. \tag{14}$$

Similarly, one can obtain the time signals emitted by array 1 or received on array 2 with all the focusing techniques studied previously in this paper. Thus, these techniques are compared in Fig. 3(b), (d), and (e) for cylindrical laws, time reversal, and inverse filter. Note that no postprocessing deconvolution has been used. In fact, the propagation medium itself acts as a deconvoluting medium. The inverse filter takes advantage of the broadband defocusing effect due to the medium. These results clearly highlight the fact that, in complex media, short pulses may not always be the best signals in order to obtain a short time signal in the focal plane.

V. From Time Reversal to Inverse Filter

It has been shown that in heterogeneous dissipative media, a time-reversal mirror does not achieve an optimum focusing, contrary to inverse-filter focusing. In fact, the signals $F_1(\omega)$ received after this first step process at each frequency in the focal plane [Fig. 4(a) and (b)] on the control points are given by (5):

$$F_1(\omega) = \mathbf{H}(\omega)\mathbf{H}^\dagger(\omega)S^*(\omega), \tag{15}$$

$F_1(\omega)$ is different from the ideal focusing $S(\omega)$ that is aimed in the focal plane. But the difference between $F_1(\omega)$ and $S(\omega)$ can be evaluated:

$$D_1(\omega) = S(\omega) - F_1(\omega). \tag{16}$$

The principle of the iterative process is to cancel this difference [20]. The wavefield difference is time reversed and $D_1^*(\omega)$ is transmitted by the control array [Fig. 4(c)]. The resulting wavefield propagates through the medium, and a signal $C(\omega) = {}^t\mathbf{H}(\omega)D_1^*(\omega)$ is recorded on the emitting array. This signal can be seen as a correcting wavefield that can be added after time reversal to the initial emission signals $E_1(\omega)$. This yields to a new emission signal [Fig. 4(d)]:

$$E_2(\omega) = E_1(\omega) + {}^t\mathbf{H}(\omega)D_1^*(\omega). \tag{17}$$

This emission signal is then time reversed and, after propagation in the medium, gives rise to a new focusing result on the control array:

$$F_2(\omega) = \mathbf{H}(\omega)E_2^*(\omega). \tag{18}$$

This iterative process is continued in order to correct step by step the emission signals $E_n(\omega)$:

$$\begin{cases} F_n(\omega) = \mathbf{H}(\omega)E_n^*(\omega) \\ D_n(\omega) = S(\omega) - R_n(\omega) \\ E_{n+1}(\omega) = E_n(\omega) + {}^t\mathbf{H}(\omega)D_n^*(\omega) \end{cases}, \tag{19}$$

with an initial step $E_1(\omega) = {}^t\mathbf{H}(\omega)S(\omega)$.

One can easily express $F_n(\omega)$ as a function of $S(\omega)$:

$$F_n(\omega) = \left\lfloor \mathbf{I} - \left(\mathbf{I} - \mathbf{H}(\omega)\mathbf{H}(\omega)^\dagger\right)^n \right\rfloor S(\omega). \tag{20}$$

Using the singular value decomposition, of $\mathbf{H}(\omega)$, this result can be expressed as:

$$F_n(\omega) = \mathbf{U}\left\lfloor \mathbf{I} - \left(\mathbf{I} - \mathbf{D}(\omega)\mathbf{D}(\omega)^*\right)^n \right\rfloor \mathbf{U}^\dagger S(\omega), \tag{21}$$

where $\lfloor \mathbf{I} - (\mathbf{I} - \mathbf{D}(\omega)\mathbf{D}(\omega)^*)^n \rfloor$ is a diagonal matrix whose i^{th} diagonal elements is $\mu_i = \left\lfloor 1 - \left(1 - \lambda_i^2(\omega)\right)^n \right\rfloor$.

We will consider that the propagation operator has been normalized so that $0 < \lambda_i \leq 1$.

Two cases occur:

- $0 < \lambda_i \leq 1$ and corresponds to physical signal: μ_i converges to 1,
- $\lambda_i = 0$ and corresponds to noise: μ_i is equal to 0.

$F_n(\omega)$ converges toward $F(\omega)$:

$$\lim_{\mathbf{n}\to\infty} F_n(\omega) = \mathbf{U}(\omega)\begin{bmatrix} 1 & 0 & \cdots & \cdots & \cdots & 0 \\ 0 & \ddots & 0 & & & \vdots \\ \vdots & 0 & 1 & & & \vdots \\ \vdots & & & 0 & & \vdots \\ \vdots & & & & \ddots & \vdots \\ 0 & \cdots & \cdots & \cdots & \cdots & 0 \end{bmatrix}\mathbf{U}^\dagger(\omega)S(\omega) = F(\omega). \tag{22}$$

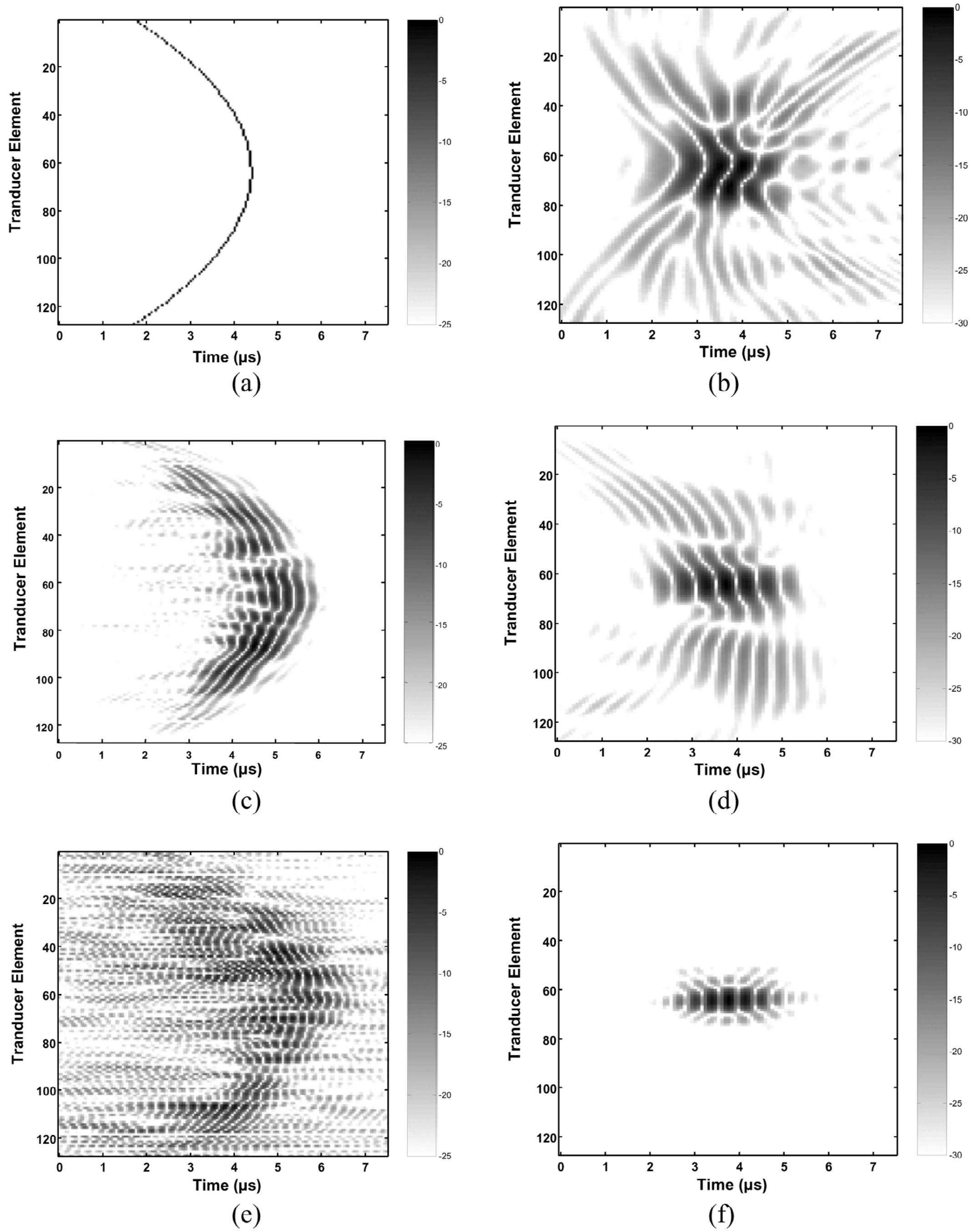

Fig. 3. Spatio-temporal focusing: emission vectors $e_i(t)_{,1\leq i\leq N}$ corresponding to a cylindrical law (a), with time reversal (c) and with the inverse filter (d); and B scan in the focal plane obtained when focusing with a cylindrical law (b), with time reversal (d) and with the inverse filter (f).

By comparing (22) to (11), one can see that the iterative process converges toward the focusing obtained with the inverse-filter technique, so that $E_n(\omega)$ converges toward the solution obtained by the inverse-filter technique $E(\omega)$.

VI. Experimental Results

The iterative time reversal process has been tested with the experimental setup described in Section II and presented in Fig. 1. Two specific aberrating media have been tested: a half human skull and a metal plate.

A. Transskull Focusing

The global effect of the skull bone on ultrasonic transcranial focusing has been discussed already in Section II (see Fig. 2). We will focus here on the transition from time-reversal to inverse-filter focusing with the iterative process. The spatio-temporal shape of the emitted signals is given for the first step of iterative process corresponding to a time-reversal focusing Fig. 5(a), for the fifth step Fig. 5(c), and the thirtieth step Fig. 5(e). In the focal plane, the side-lobe level was close to -4 dB with a cylindrical law

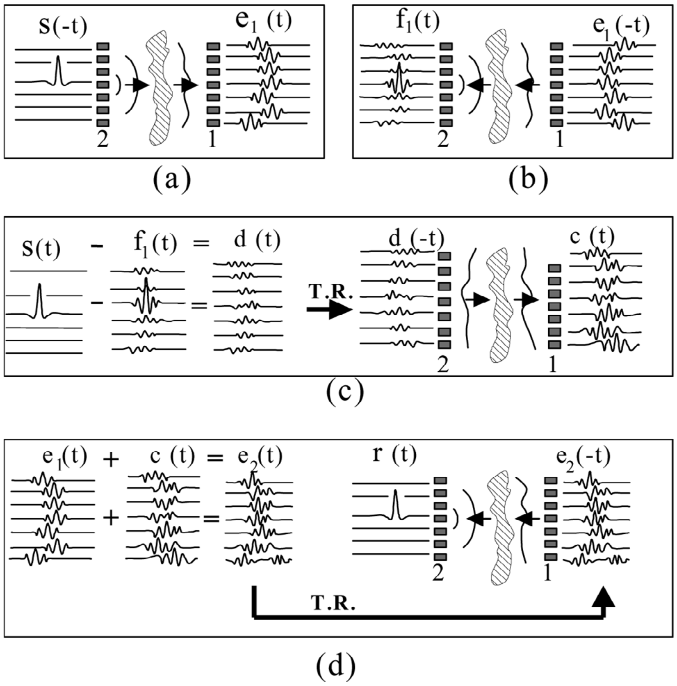

Fig. 4. The iterative method. (a) Emission of the objective pattern. (b) Focusing by time-reversal process. (c) Emission of the difference wavefield. d) Focusing with the corrected signals.

[Fig. 3(b)]. It is lowered to −7 dB with time-reversal focusing Fig. 5(b) and falls down to more than −30 dB at the thirtieth step of the iterative process [Fig. 5(f)]. The last step is quite close to the inverse-filter signals given in Fig. 3(e). Thus, a progressive transition can be seen in Fig. 5 from time-reversal to inverse-filter focusing. The corresponding B scans obtained in the focal plane also exhibit a transition from time reversal to inverse filter [respectively, in Fig. 5(b), (d) and (e) for time-reversal, step number 5 and step number 30].

Enhancing transskull focusing could have tremendous applications in ultrasonic brain imaging, particularly in the early detection of strokes. Even though the iterative process presented here requires control points in the focal plane, it is envisioned to adapt it to noninvasive transskull focusing. In this particular application, two arrays of transducers would be placed on each side of the human skull. This is currently under investigation, but it is well beyond the scope of this paper and will be presented in another paper.

B. Reverberating Echoes Cancellation

The efficacy of the iterative technique also has been tested in a reverberating medium. The aim here is to achieve precise multiple focusing through a solid plate. In the first step of the process, an impulse is emitted simultaneously by three transducers of the control array (transducers 32, 64, and 96). The signals received on the emitting array 1 are time reversed and re-emitted. The emitted signals are presented in Fig. 6(a) and the corresponding B scan obtained in the focal plane can be seen in Fig. 6(b). Three main focal spots can be seen at time 25 μs, followed and preceded by a first reflection (arriving respectively at time 17 μs and 33 μs) and a second reflection (arriving respectively at time 8 μs and 42 μs). The first reflection yields an unwanted −15 dB signal. In the case of cylindrical focusing, a similar B scan would be observed without any reflection preceding the main focal spots.

The spatio-temporal shape of the emitted signals also is given in Fig. 6 for the fifth step (c) and the thirtieth one (e). In all cases, multiple wave fronts can be seen on the emitting signals. The corresponding B scans obtained in the focal plane filter [respectively, in Fig. 6(b), (d), and (e) for time reversal, step number 5 and step number 30] show a progressive attenuation of the reverberated signals down to more than −30 dB. In order to cancel a reflection, two wavefronts have to be emitted by the array, as explained in Fig. 7 for the cancellation of a reflection on the second interface of the solid plate: wavefront two will null the reflection of wavefront one thanks to destructive interference on the first interface. Of course, the complete cancellation process is more complex as longitudinal and transverse waves have to be taken into account [14].

The ability to suppress internal echoes suggests the possibility of precise nondestructive imaging behind complex geometries such as plates, tubes, or spars, after a calibration procedure. A calibration procedure also could be used to enhance the performance of transducers or even to develop new transducer technologies exploiting multiple reflections [23].

VII. Conclusions

It has been demonstrated experimentally, in various aberrating media, that complex spatio-temporal coding can enhance the focusing quality greatly. A step-by-step transition has been obtained from time-reversal focusing to inverse-filter focusing without numerical calculation of the inversion of the propagation operator, by nulling the difference between the desired focal pattern and the obtained one. At each step, the spatio-temporal codes become more and more complicated, but both spatial and temporal shapes of the pattern obtained in the focal plane were improved at each step.

An experiment in which focusing was achieved through a metal plate proved that the iterative focusing technique was able to craft a compound wavefront capable of suppressing—by destructive interference—echoes due to intraplate reflections. A successful focusing experiment through a human skull, which combines the complications of attenuation, internal reflections, and heterogeneity, demonstrated the applicability of this new technique to extremely complex media. In order to achieve noninvasive, transcranial ultrasonic imaging, it is envisioned to use two arrays of transducers on both sides of the head, one being used as the emitting array, and the other one as the control array.

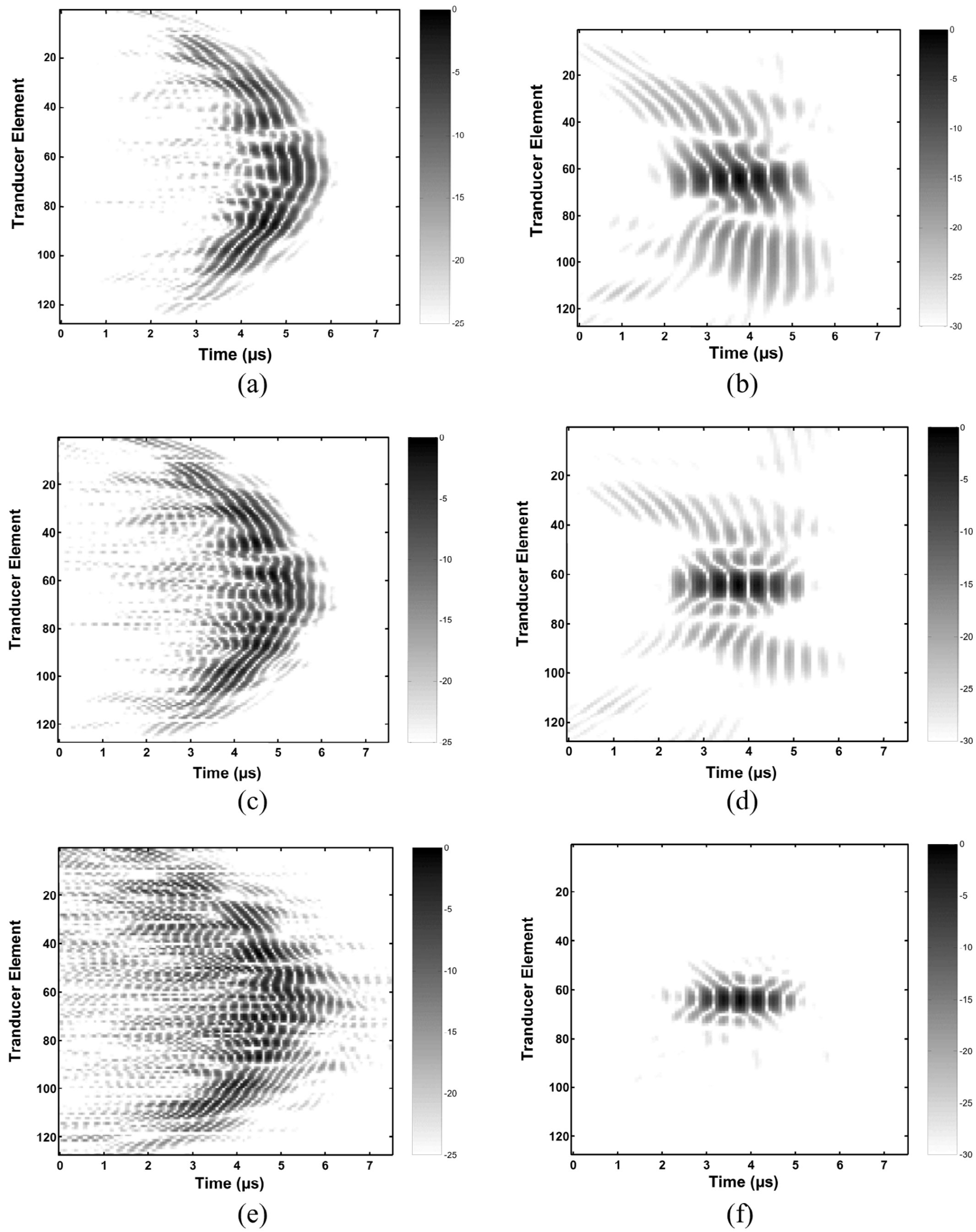

Fig. 5. Spatio-temporal focusing at several steps of the iterative process through a human skull: emission vectors $e_i(t)_{,1\leq i\leq N}$ corresponding to step 1 (a), step 5 (c), and step 30 (e). B scan in the focal plane obtained at step 1 (b), step 5 (d), and step 30 (f).

Taking advantage of the complexity of the medium, this technique demonstrates experimentally that emitting short pulses may not always be the best emitting codes in order to obtain a sharp time focusing in the focal plane. In fact, due to the heterogeneities of the medium, space and time are intimately linked, and spatio-temporal encoding is needed.

This broadband iterative focusing technique extends well beyond the experiments presented in this paper, and we believe it will find many other applications in cavities, wave-guides, multiscattering media, and more generally in various ultrasonic fields, including medical imaging, nondestructive testing, and underwater acoustics, as well as in higher frequency wave applications such as telecommunications.

References

[1] M. O'Donnell and S. W. Flax, "Phase aberration measurements in medical ultrasound: Human studies," *Ultrason. Imag.*, vol. 10, pp. 1–11, 1988.

[2] M. E. Anderson, M. S. McKeag, and G. E. Trahey, "The impact of sound speed errors on medical ultrasound imaging," *J. Acoust. Soc. Amer.*, vol. 107, pp. 3540–3548, 2000.

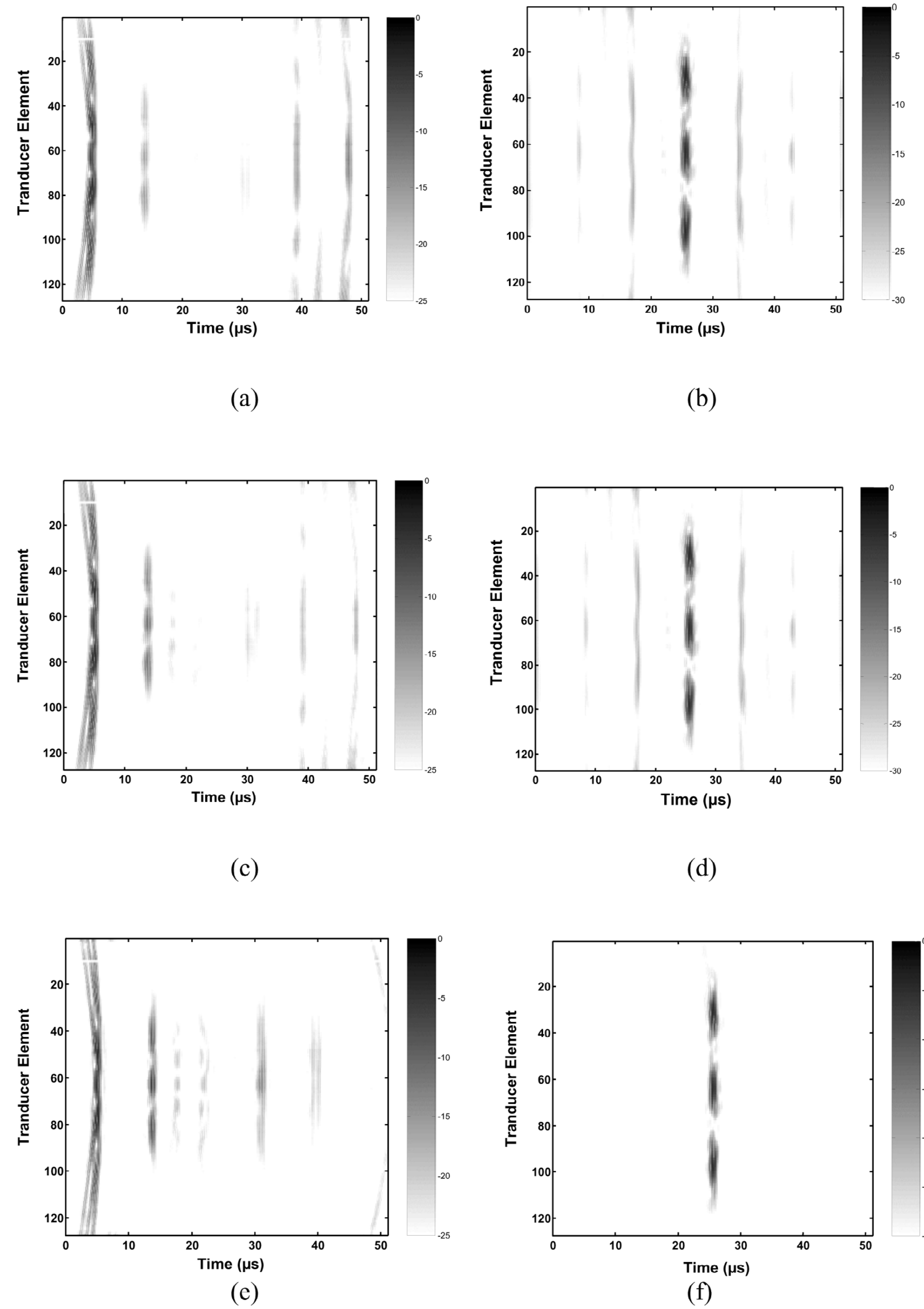

Fig. 6. Spatio-temporal focusing at several steps of the iterative process through a solid plate: emission vectors $e_i(t)_{,1\leq i\leq N}$ corresponding to step 1 (a), step 5 (c), and step 30 (e). B scan in the focal plane obtained at step 1 (b), step 5 (d), and step 30 (f).

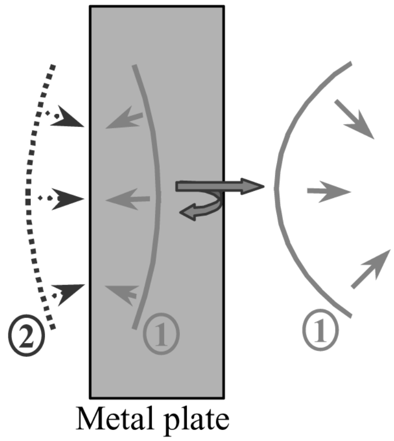

Fig. 7. Intraplate echoes cancellation.

[3] M. Moshfeghi and R. C. Waag, "In-vivo and in-vitro ultrasound beam distortion measurements of a large aperture and a conventional aperture focused transducer," *Ultrasound Med. Biol.*, vol. 14, pp. 415–428, 1988.

[4] L. Nock, G. E. Trahey, and S. W. Smith, "Phase aberration correction in medical ultrasound using speckle brightness as a quality factor," *J. Acoust. Soc. Amer.*, vol. 85, no. 5, pp. 1819–1833, 1989.

[5] D.-L. Liu and R. C. Waag, "Correction of ultrasonic wavefront distortion using backpropagation and a reference waveform method for time-shift compensation," *J. Acoust. Soc. Amer.*, vol. 96, pp. 649–660, 1994.

[6] M. O'Donnell, "Coded excitation system for improving the penetration of real-time phased-array imaging systems," *IEEE Trans. Ultrason., Ferroelect., Freq. Contr.*, vol. 39, no. 3, pp. 341–351, 1992.

[7] M. Fink, "Time reversal of ultrasonic fields—Part I: Basic principles," *IEEE Trans. Ultrason., Ferroelect., Freq. Contr.*, vol. 39, no. 5, pp. 555–566, 1992.

[8] M. Fink, "Time reversed acoustics," *Phys. Today*, vol. 20, pp. 34–40, 1997.

[9] N. Chakroun, M. Fink, and F. Wu, "Time reversal processing in non destructive testing," *IEEE Trans. Ultrason., Ferroelect., Freq. Contr.*, vol. 42, no. 2, pp. 1087–1098, 1995.

[10] H. C. Song, W. A. Kuperman, W. S. Hodgkiss, T. Akal, C. Ferla, and D. R. Jackson, "Iterative time reversal in the ocean," *J. Acoust. Soc. Amer.*, vol. 105, no. 6, pp. 3176–3184, 1999.

[11] W. A. Kuperman, W. S. Hodgkiss, H. C. Song, T. Akal, C. Ferla, and D. R. Jackson, "Phase conjugation in the ocean: Experimental demonstration of a time reversal mirror," *J. Acoust. Soc. Amer.*, vol. 103, no. 1, pp. 25–40, 1998.

[12] A. Derode, A. Tourin, J. de Rosny, M. Tanter, S. Yon, and M. Fink, "Taking advantage of multiple scattering to communicate with time reversal antennas," *Phys. Rev. Lett.*, vol. 90, no. 1, pp. 014301-1–014301-4, 2003.

[13] M. Tanter, J.-F. Aubry, J. Gerber, J.-L. Thomas, and M. Fink, "Optimal focusing by spatio-temporal inverse filter: Part I. Basic principles," *J. Acoust. Soc. Amer.*, vol. 110, no. 1, pp. 37–47, 2001.

[14] J.-F. Aubry, M. Tanter, J. Gerber, J.-L. Thomas, and M. Fink, "Optimal focusing by spatio-temporal inverse filter: Part II. Experiments," *J. Acoust. Soc. Amer.*, vol. 110, no. 1, pp. 48–58, 2001.

[15] E. Ebbini and C. Cain, "Multiple-focus ultrasound phased-array pattern synthesis: Optimal driving-signal distributions for hyperthermia," *IEEE Trans. Ultrason., Ferroelect., Freq. Contr.*, vol. 36, no. 5, pp. 540–548, 1989.

[16] H. Wang, E. Ebbini, M. O'Donnell, and C. Cain, "Phase aberration correction and motion compensation for ultrasonic hyperthermia phased arrays: Experimental results," *IEEE Trans. Ultrason., Ferroelect., Freq. Contr.*, vol. 41, no. 1, pp. 34–43, 1994.

[17] J.-F. Aubry, M. Tanter, J.-L. Thomas, and M. Fink, "Pulse echo imaging through a human skull: In vitro experiments," in *Proc. IEEE Ultrason. Symp.*, 2001, pp. 1499–1502.

[18] K. Ranganathan and W. F. Walker, "A novel beamformer design method for medical ultrasound. Part I: Theory," *IEEE Trans. Ultrason., Ferroelect., Freq. Contr.*, vol. 50, no. 1, pp. 15–24, 2003.

[19] K. Ranganathan and W. F. Walker, "A novel beamformer design method for medical ultrasound. Part II: Simulation results," *IEEE Trans. Ultrason., Ferroelect., Freq. Contr.*, vol. 50, no. 1, pp. 25–39, 2003.

[20] G. Montaldo, M. Tanter, and M. Fink, "Real time inverse filter focusing through iterative time reversal," *J. Acoust. Soc. Amer.*, vol. 115, no. 2, pp. 776–784, 2004.

[21] S. J. Norton, "Iterative inverse scattering algorithms: Methods of computing Fréchet derivatives," *J. Acoust. Soc. Amer.*, vol. 106, no. 5, pp. 2653–2660, 1999.

[22] M. Nieto-Vesperinas, *Scattering and Diffraction in Physical Optics.* New York: Wiley, 1991.

[23] G. Montaldo, D. Palacio, M. Tanter, and M. Fink, "The time reversal kaleidoscope: A new concept of smart transducers for 3D imaging," in *Proc. IEEE Ultrason. Symp.*, 2003, pp. 42–45.

Gabriel Montaldo was born 1972 in Montevideo, Uruguay. He received the Ph.D. degree in physics from the Universidad de la Republica, Uruguay, in 2001. Since 2002 he has worked in the Laboratory Ondes et Acoustique at the Ecole Supérieure de Physique et de Chimie Industrielles de la Ville de Paris (ESPCI).

His principal research includes applications of the time-reversal process to adaptive focusing in heterogeneous media, the generation of shocks waves, and telecommunications.

Jean-François Aubry was born in May 1973 in Marseille, France. He graduated in physics from Ecole Normale Superieure de Cachan and University Paris XI in 1998. In 2002, he received the Ph.D. degree in physics (acoustics) from the University of Paris VII.

Since 2002, he has had a permanent position as a researcher for the National French Center of Science (C.N.R.S). He is currently working at the Laboratoire Ondes et Acoustique, Paris, France. He is mainly working on adaptive transcranial focusing with two major medical applications: ultrasonic brain imaging and brain therapy with high intensity focused ultrasound. He holds two patents on these applications.

Mickaël Tanter was born in December 1970 in Paimpol, France. He received the Ing. degree in electronics of the Ecole Superieure d'Electricite (SUPELEC) in 1994. In 1999, he received the Ph.D. degree in physics (acoustics) from the University of Paris VII for his work on the application of time reversal to ultrasonic brain high intensity focused ultrasound (HIFU). He now has a permanent position as a researcher for the National French Center of Science (C.N.R.S) and joined in 2000 the laboratory Ondes et Acoustique (LOA) at the Ecole Supérieure de Physique et de Chimie Industrielle de la Ville de Paris (ESPCI). He is in charge of the medical applications of ultrasound at LOA.

His current research interests include wave adaptive focusing techniques in heterogeneous media, medical ultrasonic imaging, ultrasonic brain imaging, shear wave propagation in soft tissues for cancer detection, ultrasonic therapy, nonlinear acoustics, and active noise control. He holds six patents and he has published 40 articles.

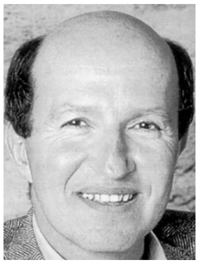

Mathias Fink received the diplome de Doctorat de 3ème cycle in solid state physics in 1970 and the Doctorat ès-Sciences degree in acoustics in 1978 from Paris University, France.

From 1981 to 1984, he was a professor of acoustics at Strasbourg University, Srasbourg, France. Since 1984, he has been a professor of physics at Paris University, Denis Diderot, France. In 1990 he founded the Laboratoire Ondes et Acoustique at the Ecole Supérieure de Physique et de Chimie Industrielles de la Ville de Paris (ESPCI). In 1994, he was elected a member of the Institut Universitaire de France.

His current research interest include medical ultrasonic imaging, ultrasonic therapy, nondestructive testing, underwater acoustics, active control of sound and vibration, analogies between optics and acoustics, wave coherence in multiple scattering media, and time reversal in physics. He has developed different techniques in speckle reduction, wave focusing in inhomogeneous media, and in ultrasonic laser generation. He holds 20 patents, and he has published more than 220 articles. In 2003, he was elected a member of the French Academy of Science.